Truth or Twist? Optimal Model Selection for Reliable Label Flipping Evaluation in LLM-based Counterfactuals

Qianli Wang 1,3,* Van Bach Nguyen 2,* Nils Feldhus 1,3,5 Luis Felipe Villa-Arenas 1,3,4 Christin Seifert 2 Sebastian Möller 1,3 Vera Schmitt 1,3

¹Quality and Usability Lab, Technische Universität Berlin ²University of Marburg ³German Research Center for Artificial Intelligence (DFKI) ⁴Deutsche Telekom ⁵BIFOLD – Berlin Institute for the Foundations of Learning and Data

Correspondence: qianli.wang@tu-berlin.de vanbach.nguyen@uni-marburg.de

Abstract

Counterfactual examples are widely employed to enhance the performance and robustness of large language models (LLMs) through counterfactual data augmentation (CDA). However, the selection of the judge model used to evaluate label flipping, the primary metric for assessing the validity of generated counterfactuals for CDA, yields inconsistent results. To decipher this, we define four types of relationships between the counterfactual generator and judge models: being the same model, belonging to the same model family, being independent models, and having an distillation relationship. Through extensive experiments involving two state-of-the-art LLM-based methods, three datasets, four generator models, and 15 judge models, complemented by a user study (n = 90), we demonstrate that judge models with an independent, non-fine-tuned relationship to the generator model provide the most reliable label flipping evaluations. Relationships between the generator and judge models, which are closely aligned with the user study for CDA, result in better model performance and robustness. Nevertheless, we find that the gap between the most effective judge models and the results obtained from the user study remains considerably large. This suggests that a fully automated pipeline for CDA may be inadequate and requires human intervention.

1 Introduction

Counterfactual examples are minimally altered versions of original inputs that flip the initial label (Miller, 2019; Ross et al., 2021; Madsen et al., 2022). They serve as a valuable approach for CDA aimed at improving model robustness and performance (Liu et al., 2021; Dixit et al., 2022; Balashankar et al., 2023; Agrawal et al., 2025). We

want to emphasize the subtle yet significant distinction between counterfactuals used for explaining model predictions and those used for CDA. In the former, the objective is to flip the model's prediction, while the goal of CDA is to flip the ground **truth label** (Figure 6 in Appendix B).² To evaluate the effectiveness and validity of the LLM-generated counterfactuals for CDA, the label flip rate (LFR) is a common metric of choice (Ge et al., 2021). It is the percentage of valid counterfactuals where the ground truth labels are flipped out of the total number of instances. LFR of counterfactuals can be evaluated using either the same model that generates the counterfactual (Bhattacharjee et al., 2024a,b; Wang et al., 2025a) or independent models (Dixit et al., 2022; Balashankar et al., 2023). The optimal strategy for selecting models to evaluate the ground-truth validity of counterfactuals remains uncertain (Figure 1). This uncertainty, in turn, hampers efforts to enhance model robustness and performance through CDA, as noisy or erroneous labels may degrade model performance.

In this work, we **first** define four types of relationships between the counterfactual generator model and the judge model: being the same model, independent models with and without fine-tuning on the target dataset, distilled models, and models from the same family (Figure 1). **Secondly**, we conduct comprehensive experiments to predict labels for counterfactuals generated by two state-of-the-art approaches across three datasets and four generator models, with 15 judge models. **Thirdly**, we undertake a user study to assess the validity of the generated counterfactuals in acquiring a ground-truth LFR.

We find that a judge model with an independent, non-fine-tuned relationship to the generator captures label flipping most effectively. Relationships

^{*}Equal Contribution.

¹Code and evaluation results are available at: https://github.com/qiaw99/truth-or-twist

²In this study, we mainly focus on the latter type of counterfactuals used for CDA.



Figure 1: A counterfactual generated by Llama3-8B, with its label evaluated by judge models with different relationships, complemented by human evaluation. The revised words are highlighted in red.

between the generator and judge models that are most aligned with the user study, lead to improved model performance and robustness. Additionally, there remains a considerable gap between the performance of the best judge models and the results observed in the user study.

2 Background and Related Work

CDA Pipeline At the start of a CDA process, LLMs generate counterfactuals using established counterfactual generation approaches (Figure 4 in Appendix A). These generated counterfactuals should subsequently be validated – either by human annotators or judge models – as invalid counterfactuals bearing incorrect labels may degrade model performance (Song et al., 2023). In practice, relying solely on human evaluation is both costly and inefficient; therefore, LLMs are commonly employed to validate the generated counterfactuals. Finally, valid counterfactuals are utilized as additional training data to enhance model performance and robustness (Yang et al., 2021; Dixit et al., 2022).

Model Selection for Label Flipping Evaluation

The literature identifies two primary ways to verify label flipping in edited inputs: (1) employing an independent model, distinct from the one producing counterfactuals; (2) utilizing the same LLM that generates counterfactuals, guided by

carefully constructed prompts. Prior to, and even during the widespread adoption of LLMs, encoder-only models, e.g., DeBERTa (Dixit et al., 2022), RoBERTa (Ross et al., 2021; Balashankar et al., 2023; Treviso et al., 2023) or BERT (Kaushik et al., 2020; Fern and Pope, 2021; Robeer et al., 2021), were predominantly used to verify label flipping. This preference stems from their superior performance in text classification tasks. In more recent work, the same LLMs are increasingly employed both to generate counterfactuals (Bhattacharjee et al., 2024a,b; Wang et al., 2025a; Dehghanighobadi et al., 2025) and to evaluate them for label flipping, since their classification accuracy rivals that of fine-tuned encoder-only models.

3 Problem Framing

3.1 Label Flipping

Given that counterfactual examples used for CDA are defined as edited inputs that alter *ground truth* labels, LFR is positioned as the primary evaluation metric for assessing the effectiveness and validity of generated counterfactuals (Kaushik et al., 2020; Dixit et al., 2022; Zhu et al., 2023; Chen et al., 2023). LFR is quantified as the percentage of instances in which labels are successfully flipped relative to the total number of counterfactuals, where N stands for the total number of counterfactuals, y_k represents the ground-truth label of the original input, y_k' denotes the prediction of its correspond-

ing counterfactual and 1 is the indicator function:

$$LFR = \frac{1}{N} \sum_{n=1}^{N} \mathbb{1}(y'_{k} \neq y_{k})$$

3.2 Relationships

To determine the optimal model selection strategy for label flip evaluation, we identified four prevalent relationships $\mathcal{R}(\mathcal{G}, \mathcal{J})$ between the generator model $LLM_{\mathcal{G}}$ and judge models $LLM_{\mathcal{J}}$ (Figure 1), which are used to assess label flipping:

- Same model (\mathcal{R}_{sm}) : the two models are same. $LLM_{\mathcal{G}} = LLM_{\mathcal{J}}$
- Same model family (\mathcal{R}_{sf}) : the two models originate from the same model family $\mathcal{F}(\mathcal{M})$. $LLM_{\mathcal{G}}, LLM_{\mathcal{J}} \in \mathcal{F}(\mathcal{M})$
- Independent models (\mathcal{R}_{im}) : the two models belong to different model families.

$$LLM_{\mathcal{G}} \in \mathcal{F}(\mathcal{M}_1), LLM_{\mathcal{J}} \in \mathcal{F}(\mathcal{M}_2)$$

We further distinguish the independent models based on whether $LLM_{\mathcal{J}}$ is fine-tuned on the given dataset: independent models with (\mathcal{R}_{imw}) and without (\mathcal{R}_{imwo}) fine-tuning.

• **Distilled models** (\mathcal{R}_{dm}): $LLM_{\mathcal{G}}$ and $LLM_{\mathcal{J}}$ have an equal number of parameters and the same architecture. $LLM_{\mathcal{J}}$ is distilled and fine-tuned using synthetic data from a third model $LLM_{\mathcal{D}}$, which is more powerful and not part of the model family $\mathcal{F}(\mathcal{M})$ of the generator and judge model.

$$LLM_{\mathcal{D}} \notin \mathcal{F}(\mathcal{M})$$

$$\operatorname{Size}(LLM_{\mathcal{J}}) = \operatorname{Size}(LLM_{\mathcal{G}})$$

$$\operatorname{Archit.}(LLM_{\mathcal{J}}) = \operatorname{Archit.}(LLM_{\mathcal{G}})$$

$$LLM_{\mathcal{J}} = \operatorname{Inherit}(LLM_{\mathcal{D}})$$

$$\{LLM_{\mathcal{G}}, LLM_{\mathcal{J}}\} \cap LLM_{\mathcal{D}} = \varnothing$$

4 Experimental Setup

4.1 Counterfactual Methods Selection

We select two state-of-the-art approaches based on LLMs that are shown to generate counterfactual examples efficiently and effectively: FIZLE (Bhattacharjee et al., 2024a) and FLARE (Bhattacharjee et al., 2024b). FIZLE first prompts LLMs to identify key words within the input and then leverages these words to guide the generation of counterfactual examples. Meanwhile, FLARE generates counterfactuals by prompting LLMs in three steps: extracting latent features, identifying relevant words linked to those features, and modifying these words to produce counterfactual examples.

4.2 Datasets

We use three widely studied classification tasks for counterfactual generation in the literature³: *news topic classification*, *sentiment analysis*, and *natural language inference*.

AG News (Zhang et al., 2015) is designed for news topic classification and comprises news articles categorized into four distinct topics: *World*, *Sports*, *Business*, and *Science/Technology*.

SST2 (Socher et al., 2013) serves as a popular dataset for sentiment analysis, sourced from movie reviews. It consists of reviews annotated with binary sentiment labels: *positive* or *negative*.

SNLI (Bowman et al., 2015) is a dataset for natural language inference and contains premise–hypothesis pairs, annotated with one of three relational categories: *entailment*, *contradiction*, or *neutral*.

4.3 Models

We select four LLMs varying in parameter size - Qwen2.5- $\{14B,32B\}$ (Qwen, 2024), Llama3-{8B,70B} (AI@Meta, 2024) – to generate counterfactuals and serve as judge models $LLM_{\mathcal{J}}$ as \mathcal{R}_{sm} relationship (§3.2). Additionally, we deploy fine-tuned BERT (Devlin et al., 2019) and RoBERTa (Liu et al., 2020) on the target datasets (§4.2), along with off-the-shelf Phi4-14B (Abdin et al., 2024), Qwen2.5-72B (Qwen, 2024), Mistral-Large-Instruct (Jiang et al., 2023), DeepSeek-R1-Distill-{Qwen,Llama} (DeepSeek-AI, 2025), and Gemini-1.5-pro (Gemini, 2024) as $LLM_{\mathcal{I}}^{4}$ (Table 3). We further ensemble label flipping results from all judge models via majority voting to yield final labels (ensemble in Figure 2). Moreover, since $LLM_{\mathcal{I}}$ are used to identify label flipping, we evaluate their downstream task performance in terms of classification accuracy across three datasets: $LLM_{\mathcal{J}}$ with \mathcal{R}_{imw} relationship (BERT and RoBERTa) generally achieve the highest downstream performance (Appendix D).

4.4 User Study

We recruit 90 native English speakers and, for each of the three datasets, randomly sample 45 indices.

³Examples of the dataset and the label distribution are included in Appendix B.

⁴Detailed information about the models employed is provided in Appendix C, and the downstream task performance of each model across three datasets and the classification prompts used are presented in Appendix D.

For each subset, i.e., a generator-dataset pair (Table 3 in Appendix G), the counterfactuals generated by the corresponding generator model $LLM_{\mathcal{G}}$ for the selected indices are evaluated by two human annotators. If no majority label emerges from the labels provided by human annotators, we break the tie ourselves by selecting one of the two annotated labels, ensuring the ground-truth label is agreed upon by two people.⁵ Each annotator is given 15 counterfactuals, along with the set of possible labels given by the dataset, and tasked with selecting the optimal label. We report an inter-annotator agreement of Cohen's $\kappa = 0.55.6$ Lastly, we calculate the ground-truth LFR as the proportion of valid counterfactuals relative to the total number of instances (Table 4 in Appendix G).

4.5 Automatic Evaluation

4.5.1 Counterfactual LFR Evaluation

LFR is evaluated based on the classification results of counterfactual examples (§3.1) generated using FIZLE and FLARE (§4.1), using the deployed judge models $LLM_{\mathcal{T}}$ described in Section 4.3.

4.5.2 Human Alignment Evaluation

To assess the alignment of $LLM_{\mathcal{J}}$ with human annotators, we employ three measures: (1) the average ranking $(rank\downarrow$, Figure 2); (2) the ratio of most-to-least alignment $(r_{m/l}\uparrow)$; (3) Pearson correlation ρ between human evaluation results and LFR results by judge models.

Average Ranking To obtain the rankings, we first calculate LFR for human annotators and for each judge-generator model pair on each set of counterfactuals generated by given generator models, as reported in Table 4 of Appendix G. Next, we compute the difference (Δ) between the human LFR and the LFR of each pair. A smaller difference indicates a better ranking (lower ranking value). This process results in a ranking for each judge-generator pair. Since these pairs correspond

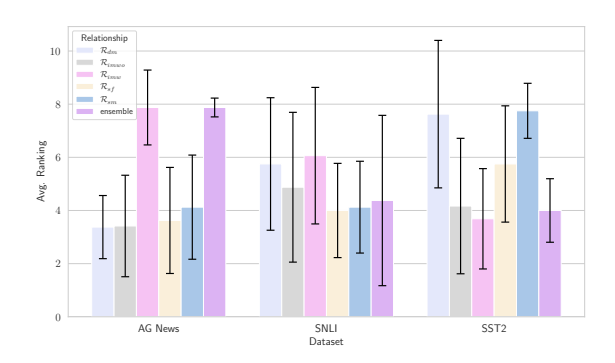


Figure 2: The average ranking of judge-generator model relationship based on Δ from Table 4 in Appendix G (lower rankings indicate better alignment). Counterfactual examples are generated by Qwen2.5-{14B,32B} and Llama3-{8B,70B}, evaluated across judge models exhibiting same, distilled, same family, ensemble, and independent w/ and w/o fine-tuning relationships on AG News, SNLI and SST2.

to specific relationships $\mathcal{R}(\mathcal{G},\mathcal{J})$, we average the rankings of all pairs sharing the same relationship to obtain the average ranking per relationship, as shown in Table 3 of Appendix G. Finally, we average these rankings for each generator model to produce the overall average rankings presented in Figure 2.

Most-to-Least-Alignment Instead of measuring overall alignment, $r_{m/\ell}$ reports how many times each relationship $\mathcal{R}_{\mathcal{G},\mathcal{J}}$ most or least closely aligned with human annotators across the three datasets:

$$r_{m/\ell}(\mathcal{R}) = \frac{1}{|\mathcal{D}|} \sum_{d \in \mathcal{D}} \frac{\mathcal{N}_{\max}(\mathcal{R}, d)}{\mathcal{N}_{\min}(\mathcal{R}, d)}$$

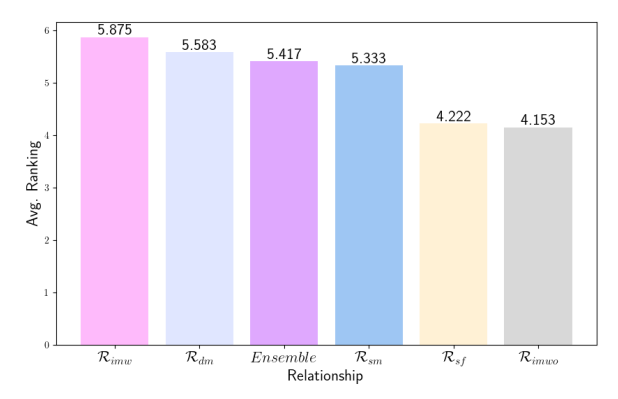
where \mathcal{D} is the set of datasets and \mathcal{N}_{max} and \mathcal{N}_{min} denote the number of cases, in which a generator-judge model pair is the most closely and least aligned with human evaluation results, respectively. A higher $r_{m/l}$ reflects better alignment.

5 Results

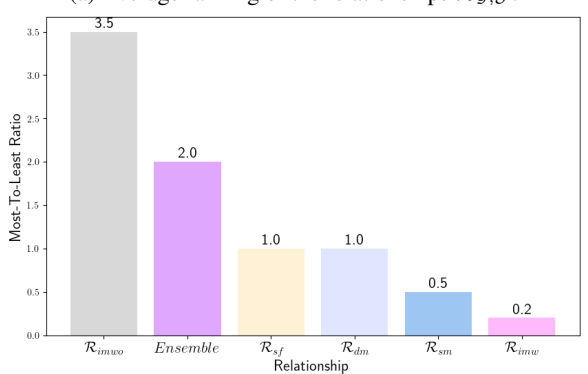
Judge model performance depends on its relationship to the generator. As shown in Figure 3a and Figure 3b, $LLM_{\mathcal{J}}$ with \mathcal{R}_{imwo} relationship achieves the highest alignment with human annotators $(rank=4.15, r_{m/l}=3.5, \rho=0.47)$. In contrast, \mathcal{R}_{dm} $(rank=5.58, r_{m/l}=1, \rho=0.38)$ or \mathcal{R}_{imw} $(rank=5.86, r_{m/l}=0.23, \rho=0.29)$ demonstrate poor alignment with human judgments. This can be attributed to data contamination

⁵The annotation guidelines and annotator information are provided in Appendix E. We further conduct an automatic evaluation in Appendix G.3 on the selected 45 counterfactuals as a sanity check to validate their **representativeness of the overall distribution**.

⁶Although we employ two state-of-the-art methods – FIZLE and FLARE – to generate counterfactuals, they are not consistently perfect (at times failing to fully shift the semantics from the original to the target label) and sometimes produce ambiguous cases (Figure 12). This has an effect on the IAA being moderate which would likely improve with the development and use of more advanced counterfactual generation methods.



(a) Average ranking of the relationships $\mathcal{R}_{\mathcal{G},\mathcal{J}}$.



(b) Most-to-least ratio $(r_{m/\ell})$ of the relationships $\mathcal{R}_{\mathcal{G},\mathcal{J}}$.

Figure 3: Average ranking and most-to-least ratio for the relationships $\mathcal{R}_{\mathcal{G},\mathcal{J}}$: same, distilled, same family, ensemble, and independent w/ and w/o fine-tuning.

(Li et al., 2025), as these models are either fine-tuned on the target dataset or share architectural similarities with $LLM_{\mathcal{G}}$. Such overlap could bias $LLM_{\mathcal{J}}$ in its evaluation of label flipping, potentially leading to either overestimating or underestimating the LFR. Notably, ensembling results from all judge models does not necessarily lead to better alignment, as it partially relies on results from suboptimal judge models. Additionally, we find that the first two measures (average ranking and $r_{m/\ell}$) are moderately correlated, with a Spearman correlation coefficient of 0.67, indicating that $r_{m/\ell}$ also serves as a reliable metric to capture the alignment between model pairs and human judgments.

High downstream performance does not necessarily indicate an effective judge model. Despite $LLM_{\mathcal{J}}$ with \mathcal{R}_{dm} or \mathcal{R}_{imw} relationships achieving the highest downstream task performance across the target datasets (Table 2 in Appendix D), their alignment with human annotators in evaluating label flipping remains considerably weak (Figure 2, Appendix G). This contrast highlights that strong downstream task performance

does not lead to reliable label flipping evaluation, and it underscores the need for careful judge model selection.

Identifying label flipping remains highly challenging. LLMs may struggle to capture nuanced changes when determining the label of imperfect counterfactuals, as the context may not have fully shifted to support a different label, resulting in ambiguity (Figure 1, Appendix F). Notably, even the optimal judge model fails to fully capture label flipping, exhibiting an average discrepancy of 22.78% relative to the user study results (Table 4 in Appendix G), which implies that a fully automated CDA pipeline is insufficient and necessitates human oversight.

Relationship $\mathcal{R}(\mathcal{G}, \mathcal{J})$ impacts CDA outcomes. We investigate how the choice of relationship affects CDA outcomes (Appendix H). We notice that when the LFR of $LLM_{\mathcal{I}}$, due to its relationship to $LLM_{\mathcal{G}}$, aligns more closely with user study outcomes, the labels identified by $LLM_{\mathcal{J}}$ are associated with improved performance and greater robustness on both unseen and out-of-distribution data (Kaushik et al., 2020; Gardner et al., 2020) (Appendix H). This association is particularly evident when these identified labels are treated as the ground-truth labels for counterfactuals, which subsequently serve as data points for CDA. This can be attributed to the fact that noisy and incorrect labels provided by judge models with suboptimal relationships contribute to performance deterioration (Zhu et al., 2022; Song et al., 2023).

6 Conclusion

In this work, we emphasize the importance of the relationship between the counterfactual generator model and label flipping judge model in achieving LFR that align more closely with human annotations and in improving CDA outcomes. We further demonstrate that high downstream performance does not necessarily imply an effective judge model. Through extensive experiments, we identify that label flipping remains highly challenging across all selected tasks. Additionally, the gap between the optimal relationship and the user study is considerably large, which indicates full automation of CDA falls short and human intervention should be considered.

Limitations

Our experimental work is confined to Englishlanguage datasets. Consequently, the effectiveness in other languages may not be comparable. Extending experiments to the multilingual setting is considered as future work.

In our experiments, we exclusively use models from Qwen and Llama families to generate counterfactuals, as from DeepSeek-R1 (DeepSeek-AI, 2025) distilled Qwen2.5 and Llama3 models are officially provided⁷ and can be used out-of-thebox. Additional work is required when employing models from a different model family as $LLM_{\mathcal{C}}$, including using DeepSeek-R1 to generate synthetic data and fine-tuning $LLM_{\mathcal{G}}$ to derive $LLM_{\mathcal{J}}$ with distillation relationships. Between the model families (Qwen, Llama, Mistral, DeepSeek), there are lots of architectural equivalences and similarities, e.g., the same attention (grouped-query attention), position embeddings (RoPE), normalization (RM-SNorm) or FFN activation (SwiGLU). We argue that, based on our comprehensive experiments and large-scale user study (n = 90), our results are considerably robust and generalizable given the similar architectures compared to other model families.

For label flipping evaluation, we select RoBERTa, BERT, Phi4-14B, Mistral-Large-Instruct-2411 Gemini-1.5-pro as representatives of independent (\mathcal{R}_{imw} , §3.2) LLMs with different parameter sizes, without comprehensively assessing models from all other widely known model families. In particular, we evaluate only open-source models, rather than closed-source, proprietary models.

Beyond LFR, counterfactuals can be evaluated subjectively – via human judgment or LLM-as-a-Judge – along dimensions such as **coherence**, **understandability**, **feasibility**, **fairness**, and **completeness** (Nguyen et al., 2024; Domnich et al., 2025; Wang et al., 2025b). While automated metrics exist for other aspects (e.g., similarity, diversity), in this paper we focus on identifying which generator–judge relationship is preferable for verifying label flipping, as informed by our user-study results.

Ethics Statement

The participants in our user studies were compensated at or above the minimum wage in accordance

with the standards of our host institutions' regions. The annotation took each annotator 45 minutes on average.

Acknowledgment

We thank Leonhard Hennig for his review of an earlier paper draft of our paper. We are indebted to the anonymous reviewers of INLG 2025 for their helpful and rigorous feedback. This work has been supported by the Federal Ministry of Research, Technology and Space (BMFTR) as part of the projects newspolygraph (03RU2U151C), BIFOLD 24B and VERANDA (16KIS2047).

References

Marah Abdin, Jyoti Aneja, Harkirat Behl, Sébastien Bubeck, Ronen Eldan, Suriya Gunasekar, Michael Harrison, Russell J. Hewett, Mojan Javaheripi, Piero Kauffmann, James R. Lee, Yin Tat Lee, Yuanzhi Li, Weishung Liu, Caio C. T. Mendes, Anh Nguyen, Eric Price, Gustavo de Rosa, Olli Saarikivi, Adil Salim, Shital Shah, Xin Wang, Rachel Ward, Yue Wu, Dingli Yu, Cyril Zhang, and Yi Zhang. 2024. Phi-4 technical report. *Preprint*, arXiv:2412.08905.

Aryan Agrawal, Lisa Alazraki, Shahin Honarvar, Thomas Mensink, and Marek Rei. 2025. Enhancing LLM robustness to perturbed instructions: An empirical study. In *ICLR 2025 Workshop on Building Trust in Language Models and Applications*.

AI@Meta. 2024. Llama 3 model card.

Ananth Balashankar, Xuezhi Wang, Yao Qin, Ben Packer, Nithum Thain, Ed Chi, Jilin Chen, and Alex Beutel. 2023. Improving classifier robustness through active generative counterfactual data augmentation. In *Findings of the Association for Computational Linguistics: EMNLP 2023*, pages 127–139, Singapore. Association for Computational Linguistics.

Amrita Bhattacharjee, Raha Moraffah, Joshua Garland, and Huan Liu. 2024a. Zero-shot LLM-guided Counterfactual Generation: A Case Study on NLP Model Evaluation. In 2024 IEEE International Conference on Big Data (BigData), pages 1243–1248, Los Alamitos, CA, USA. IEEE Computer Society.

Amrita Bhattacharjee, Raha Moraffah, Joshua Garland, and Huan Liu. 2024b. Towards llm-guided causal explainability for black-box text classifiers. In AAAI 2024 Workshop on Responsible Language Models, Vancouver, BC, Canada.

Samuel R. Bowman, Gabor Angeli, Christopher Potts, and Christopher D. Manning. 2015. A large annotated corpus for learning natural language inference. In *Proceedings of the 2015 Conference on Empirical Methods in Natural Language Processing*, pages

⁷https://huggingface.co/collections/ deepseek-ai/deepseek-r1-678e1e131c0169c0bc89728d

- 632–642, Lisbon, Portugal. Association for Computational Linguistics.
- Zeming Chen, Qiyue Gao, Antoine Bosselut, Ashish Sabharwal, and Kyle Richardson. 2023. DISCO: Distilling counterfactuals with large language models. In *Proceedings of the 61st Annual Meeting of the Association for Computational Linguistics (Volume 1: Long Papers)*, pages 5514–5528, Toronto, Canada. Association for Computational Linguistics.
- DeepSeek-AI. 2025. Deepseek-r1: Incentivizing reasoning capability in llms via reinforcement learning. *Preprint*, arXiv:2501.12948.
- Zahra Dehghanighobadi, Asja Fischer, and Muhammad Bilal Zafar. 2025. Can llms explain themselves counterfactually? *Preprint*, arXiv:2502.18156.
- Jacob Devlin, Ming-Wei Chang, Kenton Lee, and Kristina Toutanova. 2019. BERT: Pre-training of deep bidirectional transformers for language understanding. In Proceedings of the 2019 Conference of the North American Chapter of the Association for Computational Linguistics: Human Language Technologies, Volume 1 (Long and Short Papers), pages 4171–4186, Minneapolis, Minnesota. Association for Computational Linguistics.
- Tanay Dixit, Bhargavi Paranjape, Hannaneh Hajishirzi, and Luke Zettlemoyer. 2022. CORE: A retrieve-thenedit framework for counterfactual data generation. In *Findings of the Association for Computational Linguistics: EMNLP 2022*, pages 2964–2984, Abu Dhabi, United Arab Emirates. Association for Computational Linguistics.
- Marharyta Domnich, Julius Välja, Rasmus Moorits Veski, Giacomo Magnifico, Kadi Tulver, Eduard Barbu, and Raul Vicente. 2025. Towards unifying evaluation of counterfactual explanations: Leveraging large language models for human-centric assessments. *Proceedings of the AAAI Conference on Artificial Intelligence*, 39(15):16308–16316.
- Xiaoli Fern and Quintin Pope. 2021. Text counterfactuals via latent optimization and Shapley-guided search. In *Proceedings of the 2021 Conference on Empirical Methods in Natural Language Processing*, pages 5578–5593, Online and Punta Cana, Dominican Republic. Association for Computational Linguistics.
- Matt Gardner, Yoav Artzi, Victoria Basmova, Jonathan Berant, Ben Bogin, Sihao Chen, Pradeep Dasigi, Dheeru Dua, Yanai Elazar, Ananth Gottumukkala, et al. 2020. Evaluating models' local decision boundaries via contrast sets. In *Findings of the Association for Computational Linguistics: EMNLP 2020*, pages 1307–1323, Online. Association for Computational Linguistics.
- Yingqiang Ge, Shuchang Liu, Zelong Li, Shuyuan Xu, Shijie Geng, Yunqi Li, Juntao Tan, Fei Sun, and Yongfeng Zhang. 2021. Counterfactual evaluation for explainable ai. *Preprint*, arXiv:2109.01962.

- Gemini. 2024. Gemini 1.5: Unlocking multimodal understanding across millions of tokens of context. *Preprint*, arXiv:2403.05530.
- Albert Q. Jiang, Alexandre Sablayrolles, Arthur Mensch, Chris Bamford, Devendra Singh Chaplot, Diego de las Casas, Florian Bressand, Gianna Lengyel, Guillaume Lample, Lucile Saulnier, Lélio Renard Lavaud, Marie-Anne Lachaux, Pierre Stock, Teven Le Scao, Thibaut Lavril, Thomas Wang, Timothée Lacroix, and William El Sayed. 2023. Mistral 7b. *Preprint*, arXiv:2310.06825.
- Divyansh Kaushik, Eduard Hovy, and Zachary Lipton. 2020. Learning the difference that makes a difference with counterfactually-augmented data. In *International Conference on Learning Representations*.
- Dawei Li, Renliang Sun, Yue Huang, Ming Zhong, Bohan Jiang, Jiawei Han, Xiangliang Zhang, Wei Wang, and Huan Liu. 2025. Preference leakage: A contamination problem in llm-as-a-judge. *Preprint*, arXiv:2502.01534.
- Qi Liu, Matt Kusner, and Phil Blunsom. 2021. Counterfactual data augmentation for neural machine translation. In *Proceedings of the 2021 Conference of the North American Chapter of the Association for Computational Linguistics: Human Language Technologies*, pages 187–197, Online. Association for Computational Linguistics.
- Yinhan Liu, Myle Ott, Naman Goyal, Jingfei Du, Mandar Joshi, Danqi Chen, Omer Levy, Mike Lewis, Luke Zettlemoyer, and Veselin Stoyanov. 2020. Ro{bert}a: A robustly optimized {bert} pretraining approach.
- Andreas Madsen, Siva Reddy, and Sarath Chandar. 2022. Post-hoc interpretability for neural nlp: A survey. *ACM Comput. Surv.*, 55(8).
- Tim Miller. 2019. Explanation in artificial intelligence: Insights from the social sciences. *Artificial intelligence*, 267:1–38.
- Van Bach Nguyen, Christin Seifert, and Jörg Schlötterer. 2024. CEval: A benchmark for evaluating counterfactual text generation. In *Proceedings of the 17th International Natural Language Generation Conference*, pages 55–69, Tokyo, Japan. Association for Computational Linguistics.
- Qwen. 2024. Qwen2.5 technical report. *Preprint*, arXiv:2412.15115.
- Marcel Robeer, Floris Bex, and Ad Feelders. 2021. Generating realistic natural language counterfactuals. In *Findings of the Association for Computational Linguistics: EMNLP 2021*, pages 3611–3625, Punta Cana, Dominican Republic. Association for Computational Linguistics.
- Alexis Ross, Ana Marasović, and Matthew Peters. 2021. Explaining NLP models via minimal contrastive editing (MiCE). In *Findings of the Association for Computational Linguistics: ACL-IJCNLP 2021*, pages

3840–3852, Online. Association for Computational Linguistics.

Richard Socher, Alex Perelygin, Jean Wu, Jason Chuang, Christopher D. Manning, Andrew Ng, and Christopher Potts. 2013. Recursive deep models for semantic compositionality over a sentiment treebank. In *Proceedings of the 2013 Conference on Empirical Methods in Natural Language Processing*, pages 1631–1642, Seattle, Washington, USA. Association for Computational Linguistics.

Hwanjun Song, Minseok Kim, Dongmin Park, Yooju Shin, and Jae-Gil Lee. 2023. Learning from noisy labels with deep neural networks: A survey. *IEEE transactions on neural networks and learning systems*, 34(11):8135—8153.

Marcos Treviso, Alexis Ross, Nuno M. Guerreiro, and André Martins. 2023. CREST: A joint framework for rationalization and counterfactual text generation. In *Proceedings of the 61st Annual Meeting of the Association for Computational Linguistics (Volume 1: Long Papers)*, pages 15109–15126, Toronto, Canada. Association for Computational Linguistics.

Sowmya Vajjala and Shwetali Shimangaud. 2025. Text classification in the llm era - where do we stand? *Preprint*, arXiv:2502.11830.

Qianli Wang, Nils Feldhus, Simon Ostermann, Luis Felipe Villa-Arenas, Sebastian Möller, and Vera Schmitt. 2025a. FitCF: A framework for automatic feature importance-guided counterfactual example generation. In *Findings of the Association for Computational Linguistics: ACL 2025*, pages 1176–1191, Vienna, Austria. Association for Computational Linguistics.

Qianli Wang, Mingyang Wang, Nils Feldhus, Simon Ostermann, Yuan Cao, Hinrich Schütze, Sebastian Möller, and Vera Schmitt. 2025b. Through a compressed lens: Investigating the impact of quantization on llm explainability and interpretability. *Preprint*, arXiv:2505.13963.

Linyi Yang, Jiazheng Li, Padraig Cunningham, Yue Zhang, Barry Smyth, and Ruihai Dong. 2021. Exploring the efficacy of automatically generated counterfactuals for sentiment analysis. In *Proceedings of the 59th Annual Meeting of the Association for Computational Linguistics and the 11th International Joint Conference on Natural Language Processing (Volume 1: Long Papers)*, pages 306–316, Online. Association for Computational Linguistics.

Xiang Zhang, Junbo Zhao, and Yann LeCun. 2015. Character-level convolutional networks for text classification. In *Advances in Neural Information Processing Systems*, volume 28. Curran Associates, Inc.

Dawei Zhu, Michael A. Hedderich, Fangzhou Zhai,
David Ifeoluwa Adelani, and Dietrich Klakow. 2022.
Is BERT robust to label noise? a study on learning with noisy labels in text classification. In *Proceedings of the Third Workshop on Insights from Negative*

Results in NLP, pages 62–67, Dublin, Ireland. Association for Computational Linguistics.

Yingjie Zhu, Jiasheng Si, Yibo Zhao, Haiyang Zhu, Deyu Zhou, and Yulan He. 2023. EXPLAIN, EDIT, GENERATE: Rationale-sensitive counterfactual data augmentation for multi-hop fact verification. In *Proceedings of the 2023 Conference on Empirical Methods in Natural Language Processing*, pages 13377–13392, Singapore. Association for Computational Linguistics.

A Counterfactual Data Augmentation Pipeline

Figure 4 illustrates the CDA pipeline. LLMs first generate counterfactuals using counterfactual generation approaches such as FIZLE and FLARE, both of which are used in our work (§4.1). The generated counterfactuals must then be validated—either by human annotators or judge models—as invalid counterfactuals with incorrect labels may degrade model performance (Zhu et al., 2022; Song et al., 2023). Finally, valid counterfactuals are utilized as additional training data to enhance model performance and robustness.

B Datasets

B.1 Label Distribution

Figure 5 shows the label distributions of AG News, SNLI and SST2.

B.2 Dataset Example

Figure 6 displays dataset examples from AG News, SST2 and SNLI.

C Models

Table 1 provides detailed information about deployed models in our experiments. All models were directly obtained from the Hugging Face⁸ repository. All experiments were conducted using A100 or H100 GPUs. For each model, counterfactual example generation across the entire dataset can be completed within 10 hours.

D Downstream Task Performance

Table 2 reports the downstream task performance for all LLMs presented in Table 3 and Section 4.3 on the AG News, SST2, and SNLI datasets. Zero-shot prompting is applied to

⁸https://huggingface.co/

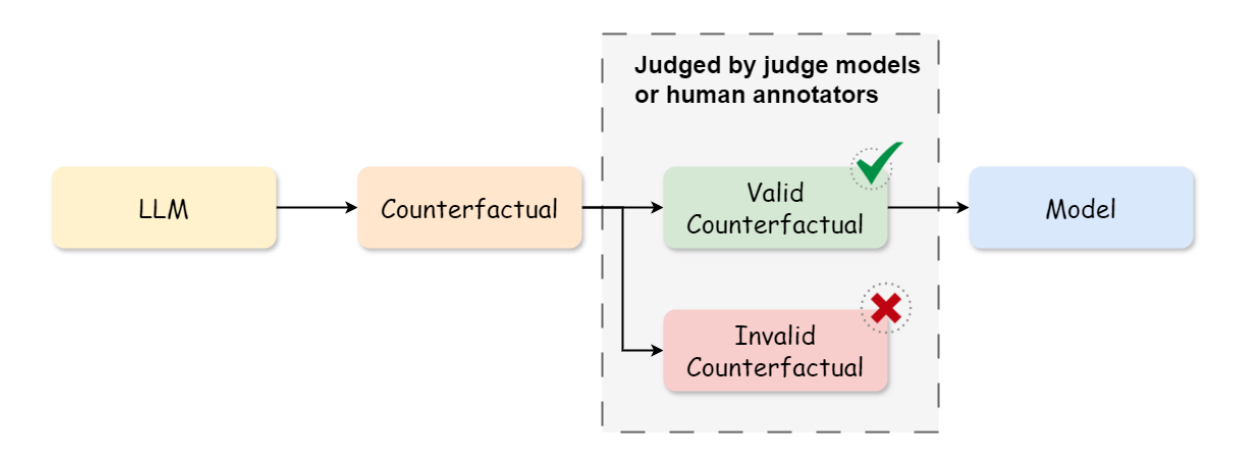


Figure 4: Counterfactual Data Augmentation pipeline.

Name	Citation	Size	Link
BERT (AG News)	Devlin et al. (2019)	110M	https://huggingface.co/textattack/bert-base-uncased-ag-news
BERT (SST2)	Devlin et al. (2019)	110M	https://huggingface.co/textattack/bert-base-uncased-SST-2
BERT (SNLI)	Devlin et al. (2019)	110M	https://huggingface.co/textattack/bert-base-uncased-snli
RoBERTa (AG News)	Liu et al. (2020)	125M	https://huggingface.co/textattack/roberta-base-ag-news
RoBERTa (SST2)	Liu et al. (2020)	125M	https://huggingface.co/textattack/roberta-base-SST-2
RoBERTa (SNLI)	Liu et al. (2020)	125M	https://huggingface.co/pepa/roberta-base-snli
Llama3	AI@Meta (2024)	8B	https://huggingface.co/meta-llama/Meta-Llama-3-8B-Instruct
Llama3	AI@Meta (2024)	70B	https://huggingface.co/meta-llama/Meta-Llama-3-70B-Instruct
Qwen2.5	Qwen (2024)	7B	https://huggingface.co/Qwen/Qwen2.5-7B-Instruct
Qwen2.5	Qwen (2024)	14B	https://huggingface.co/Qwen/Qwen2.5-14B-Instruct
Qwen2.5	Qwen (2024)	32B	https://huggingface.co/Qwen/Qwen2.5-32B-Instruct
Qwen2.5	Qwen (2024)	72B	https://huggingface.co/Qwen/Qwen2.5-72B-Instruct
Phi4	Abdin et al. (2024)	14B	https://huggingface.co/microsoft/phi-4
Mistral-Large-Instruct-2311	Jiang et al. (2023)	123B	https://huggingface.co/mistralai/Mistral-Large-Instruct-2411
Gemini-1.5-pro	Gemini (2024)	n.a.	https://gemini.google.com/
DeepSeek-R1-Distill-Qwen-14B	DeepSeek-AI (2025)	14B	https://huggingface.co/deepseek-ai/DeepSeek-R1-Distill-Qwen-14B
DeepSeek-R1-Distill-Qwen-32B	DeepSeek-AI (2025)	32B	https://huggingface.co/deepseek-ai/DeepSeek-R1-Distill-Qwen-32B
DeepSeek-R1-Distill-Llama-8B	DeepSeek-AI (2025)	8B	https://huggingface.co/deepseek-ai/DeepSeek-R1-Distill-Llama-8B
DeepSeek-R1-Distill-Llama-70B	DeepSeek-AI (2025)	70B	https://huggingface.co/deepseek-ai/DeepSeek-R1-Distill-Llama-70B

Table 1: Detailed information about used models in our experiments.

Model	AG News	SST-2	SNLI
Qwen2.5-7B	78.93	93.23	88.07
Qwen2.5-14B	82.80	93.23	82.43
Qwen2.5-32B	81.79	94.50	85.67
Qwen2.5-72B	78.30	94.38	85.60
Llama3-8B	71.00	86.70	50.93
Llama3-70B	83.10	94.15	62.70
DeepSeek-R1-Distill-Qwen-7B	76.92	78.56	58.87
DeepSeek-R1-Distill-Qwen-14B	81.95	88.90	74.33
DeepSeek-R1-Distill-Qwen-32B	83.81	93.25	79.10
DeepSeek-R1-Distill-Llama-8B	80.71	85.21	49.60
DeepSeek-R1-Distill-Llama-70B	84.81	92.15	73.02
bert-base-uncased	95.14	92.32	87.50
roberta-base-uncased	94.69	94.04	88.60
Phi4-14B	80.49	92.78	82.93
Mistral-Large	79.93	84.40	85.73
Gemini-1.5-pro	83.60	95.40	77.80

Table 2: Downstream task performance, qualified by F_1 score (in %) on the AG News, SST2 and SNLI datasets.

DeepSeek-R1-Distill-{Qwen,Llama}, as few-shot prompting consistently impairs their performance (DeepSeek-AI, 2025). Furthermore, as observed in Figure 7 and Figure 9, there is an inverse

correlation between the number of demonstrations and classification accuracy for the AG News and SNLI datasets, aligned with the finding of Vajjala and Shimangaud (2025). Similarly, in Figure 8, in-

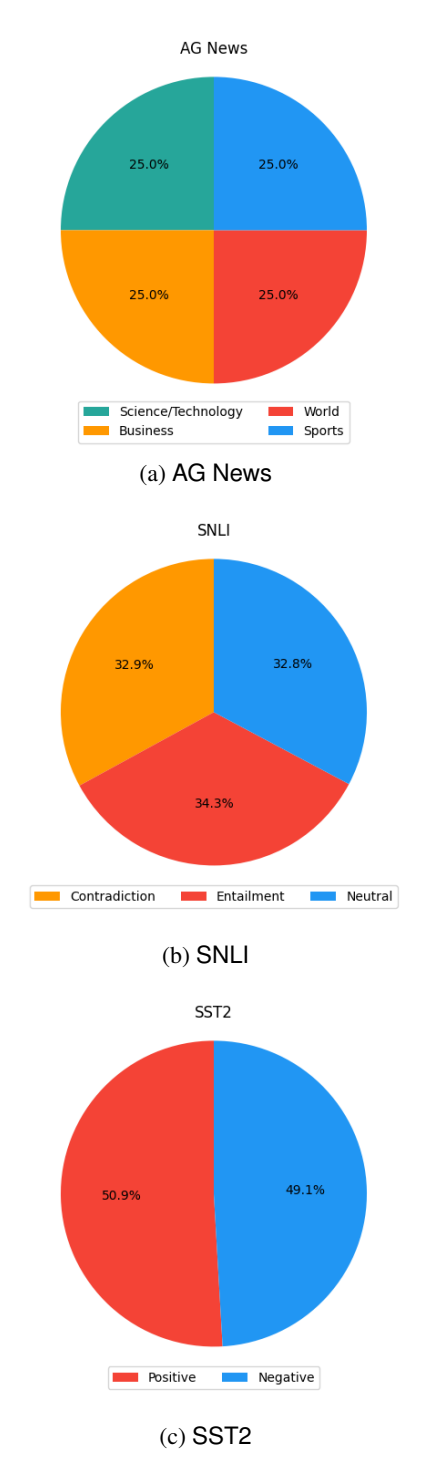


Figure 5: Label distributions of AG News, SNLI and SST2.

creasing number of demonstrations does not yield significant benefits and, in some cases, even degrades performance for the SST2 dataset. Therefore, zero-shot prompting is employed for all other decoder-only LLMs as well. The used prompt instructions are shown in Figure 10.

E Human Annotation

Figure 11 shows the annotation guideline provided to the recruited human annotators (§4.4). The counterfactuals are presented to annotators in the form of questionnaires. We use the Crowdee⁹ crowdsourcing platform to recruit annotators, distribute the questionnaires, and store their responses. A total of 90 annotators were recruited, all of whom are native English speakers without requiring specific expertise in explainable AI (XAI). Each annotators will be given 15 counterfactuals, along with a set of predefined labels depending on datasets (§4.2). Each counterfactual will be evaluated by at least two annotators.

F Challenges in Label Flipping Identification

Figure 12 displays an example from AG News, its corresponding counterfactual generated by Llama3-70B using FIZLE, and the chain-of-thought from DeepSeek-R1-Distill-Llama-70B (DeepSeek-AI, 2025) which serves as the judge model $LLM_{\mathcal{J}}$ to identify the label flipping. Underlined words are determined by Llama3-70B and newly inserted to achieve the necessary label flip.

In the given example, **business**-related terms such as "stock market" and "National Exchange" are deliberately inserted in an attempt to flip the label from **sports** to **business**. However, the sentence still centers around a baseball game, prominently featuring "Randy Johnson", a well-known professional pitcher. This kind of example introduces a unique challenge. Human evaluators may recognize Randy Johnson as a sports figure and discount the inserted business terms. In contrast, LLMs may weigh both the artificial business cues and the surrounding sports context, attempting to reconcile the conflicting signals using their implicit knowledge. This divergence can lead to different forms of error:

- Human evaluators may rely more on surfacelevel keywords and could be misled by terms like "stock market", especially if they lack specific domain knowledge.
- LLMs, on the other hand, may attempt to resolve the contradiction by grounding entities in factual knowledge, leading to confusion when contextual signals conflict.

⁹https://www.crowdee.com/

AG News (News Topic Classification)

News: E-mail scam targets police chief Wiltshire Police warns about ""phishing"" after its fraud squad chief was targeted.

Ground-truth Label: sci/tech

Counterfactual: E-mail scam targets <u>Manchester United's ticketing director</u> club warns supporters about "phishing" after its season-ticket manager was targeted.

Counterfactual label: sports

SST2 (Sentiment Analysis)

Review: Allows us to hope that nolan is poised to embark a major career as a commercial yet inventive filmmaker.

Ground-truth Label: positive

Counterfactual: <u>Dashes</u> any hope that \underline{N} olan is poised to embark on a major career as a commercial yet inventive filmmaker.

Counterfactual label: negative

SNLI (Natural Language Inference)

Premise: This church choir sings to the masses as they sing joyous songs from the book at a church.

Hypothesis: The church has cracks in the ceiling.

Ground-truth Label: neutral

Counterfactual (Hypothesis): The church is completely empty and silent.

Counterfactual label: contradiction

Figure 6: Dataset Examples from AG News, SST2 and SNLI.

Such discrepancies may explain observed patterns in the automatic evaluation (Table 3). For instance, the 100% label flip rate (LFR) by humans on counterfactuals from the SNLI dataset suggests that annotators are highly influenced by inserted keywords. Meanwhile, LLMs exhibit lower FLRs, likely due to their more nuanced, knowledge-driven reasoning process. This illustrates a key distinction in how humans and models handle ambiguous inputs: humans may overfit to superficial cues, while LLMs attempt to resolve deeper semantic inconsistencies.

Furthermore, from the reasoning chains of

DeepSeek-R1-Distill-Llama-70B in Figure 12, we observe that it becomes confused when determining whether the label of the counterfactual flips, as the context remains ambiguous despite the inclusion of additional information about the stock market. This indicates that more advanced techniques for counterfactual generation are needed, and greater attention should be devoted to this area.

G Automatic Evaluation

G.1 Average Ranking

Table 3 shows the average ranking of each judgegenerator model relationship based on Δ in Table 4.

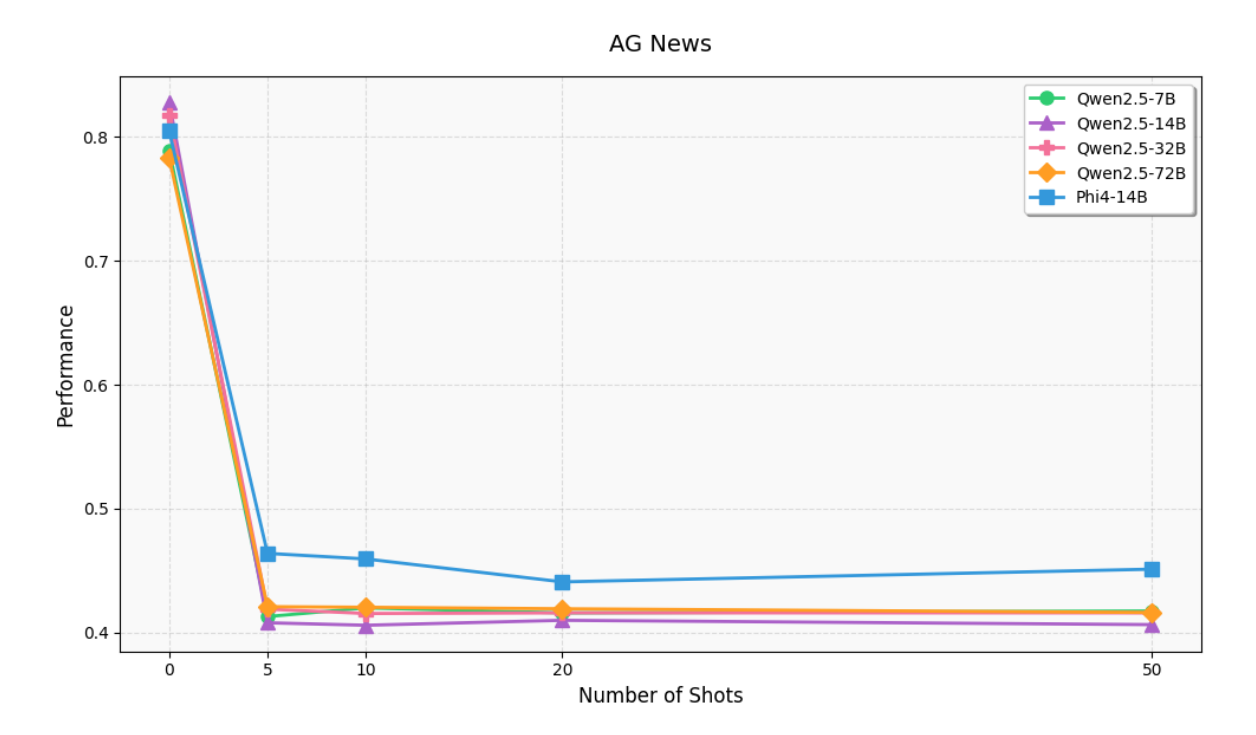


Figure 7: Classification performance of models on the AG News dataset under different few-shot learning scenarios $(n \in \{0, 5, 10, 20, 50\})$.

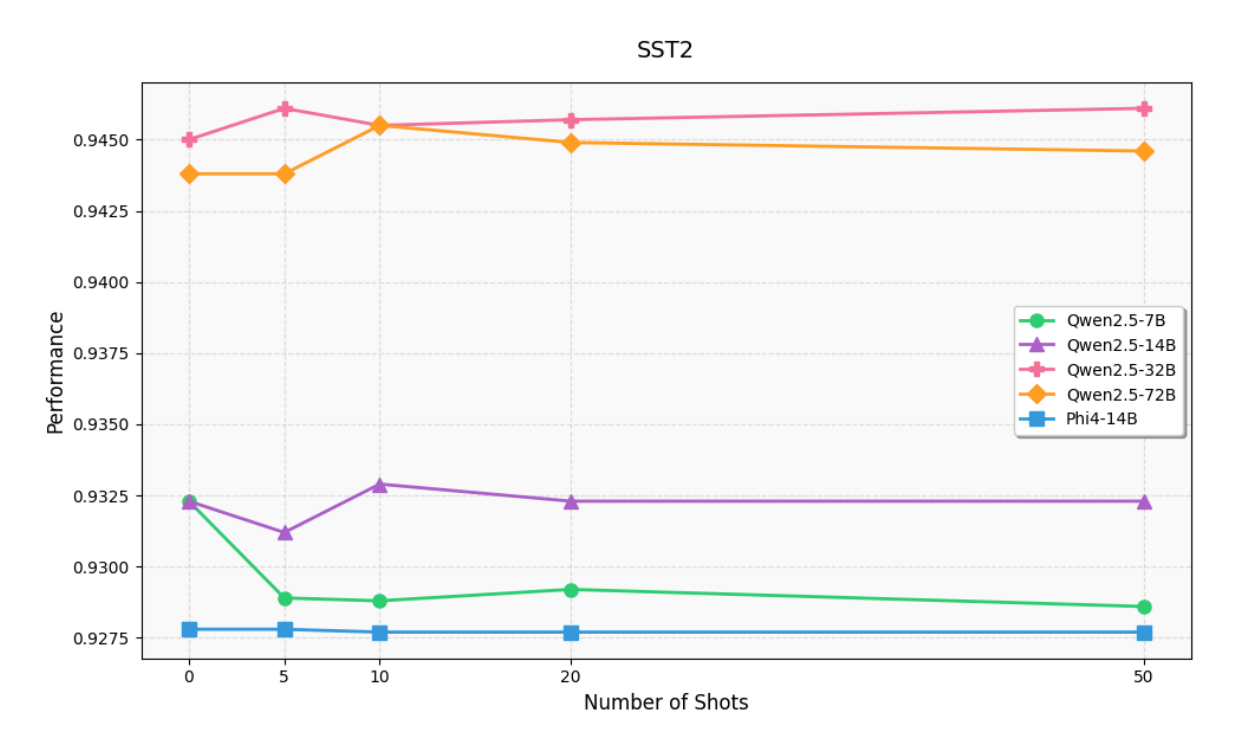


Figure 8: Classification performance of models on the SST2 dataset under different few-shot learning scenarios $(n \in \{0, 5, 10, 20, 50\})$.

Figure 3 shows the average ranking and $r_{m/\ell}$ of the relationships $\mathcal{R}_{\mathcal{G},\mathcal{J}}$. We observe that judge models with \mathcal{R}_{imwo} achieve the lowest average ranking, while those with \mathcal{R}_{imw} achieve the highest. Here, a lower ranking indicates that the corresponding

label-flipping results are more closely aligned with human evaluation outcomes.



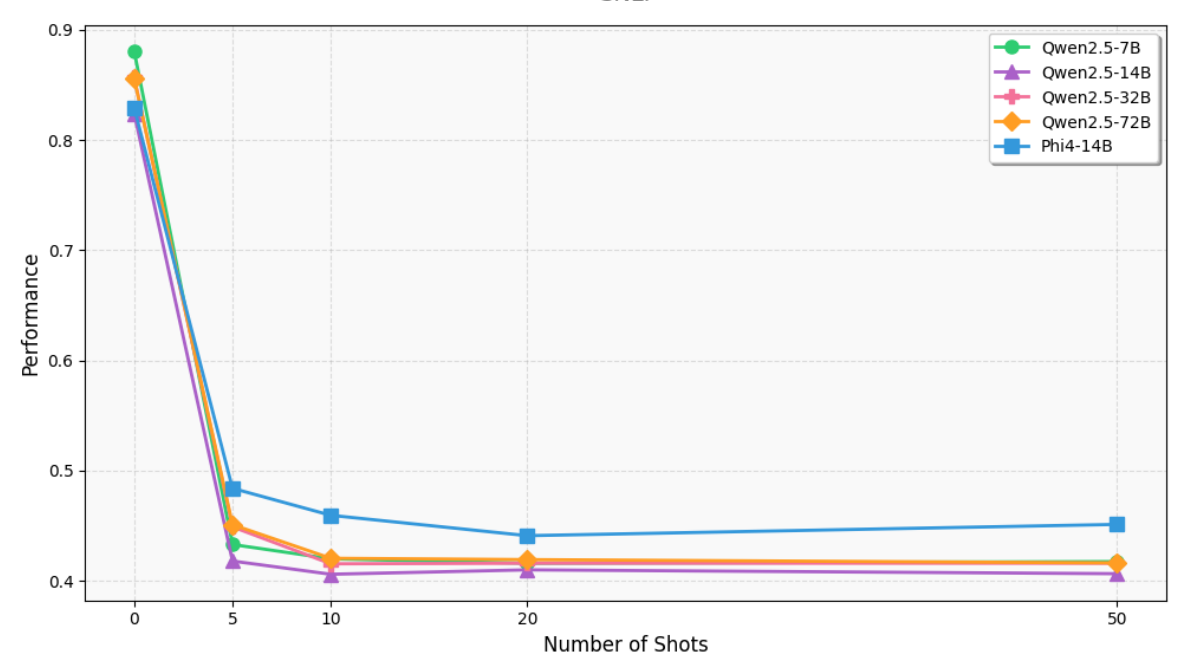


Figure 9: Classification performance of models on the SNLI dataset under different few-shot learning scenarios $(n \in \{0, 5, 10, 20, 50\})$.

Prompt Instruction for Classification on AG News

You're given an input from the AG News dataset for article topic classification. You should classify it into one of the following categories: "world", "sports", "business", or "science/technology". Output the category only!

Prompt Instruction for Classification on SST2

You're given an input from the SST2 dataset for sentiment analysis. You should classify it into one of the following categories: "positive", or "negative". Output the category only!

Prompt Instruction for Classification on SNLI

You're given a premise and a hypothesis from the SNLI dataset for natural language inference. You should classify it into one of the following categories: "neutral", "contradiction", or "entailment". Output the category only!

Figure 10: Prompt instruction for classification on AG News, SST2, and SNLI.

G.2 LFR Differences in Discrete Values

Table 4 shows the differences calculated by subtracting the user study results from the results of the judge models $LLM_{\mathcal{J}}$ results.

G.3 A Sanity Check

In our user study, we randomly select 45 counterfactuals from each dataset, generated individually by five counterfactual generator models $LLM_{\mathcal{G}}$ (§4.4). To perform a sanity check and validate the representativeness of these subsets, we conduct an additional automatic evaluation on the subset of **input data** from which the 45 counterfactuals were generated.

Table 5 outlines the LFR performance of the generated counterfactuals across the subsets of the three dataset (§4.2). We observe that the entries in

Annotation Guideline

User Study Description:

Dear participants,

Thanks for attending our user study. Our user study investigates how participants simulate model behavior based on provided explanations—an approach known as the simulatability test. You will be presented with explanations and predefined label options (depending on the dataset) and are asked to select the most appropriate label based solely on the explanations. We employ three datasets for this study: **AG News** (news topic classification), **SST-2** (sentiment analysis), and **SNLI** (natural language inference). The explanations are generated by models of varying sizes; however, model identities and sizes are not disclosed to participants.

Dataset Structure:

AG News: This dataset consists of news articles. The task is to determine whether the topic of each article pertains to one of the following categories: Sports, World, Business, or Science/Technology.

AG News Example: {example}

SST-2 (Stanford Sentiment Treebank): This dataset comprises movie reviews. The task is to assess the sentiment expressed in each review and classify it as either Positive or Negative.

SST2 Example: {example}

SNLI (Stanford Natural Language Inference): Each example consists of a premise and a hypothesis. The task is to determine the relationship between the two, categorizing it as either Entailment, Contradiction, or Neutral based on the information in the premise.

SNLI Example: {example}

Entailment means the hypothesis must be true if the premise is true. Contradiction means the hypothesis must be false if the premise is true. Neutral means the hypothesis might be true, or might not — we can't tell just from the premise.

User Study Instruction:

You will be provided with 15 instances to evaluate. Each instance includes a single input field, depending on the dataset: a news article (AG News), a movie review (SST-2), or a premise–hypothesis pair (SNLI). If the text is applicable to multiple labels, please select the most appropriate one and report them in the follow-up question. If the text is applicable to multiple labels, please select the most appropriate one and report them in the follow-up question ("Do you think the text is applicable to multiple labels? (optional)").

Figure 11: Annotation guidelines for the user study

Table 5 differ from those in Table 3, and the optimal judge model $LLM_{\mathcal{J}}$ for a given counterfactual generator model $LLM_{\mathcal{G}}$ and dataset may vary. Nevertheless, our core finding remain consistent (§5): judge models with an independent relationship without fine-tuning on the target dataset are the most effective at capturing actual label flips, as indicated by the alignment between automatic evaluation results and user study outcomes. In con-

trast, independently related judge models that have been fine-tuned on the target dataset perform the suboptimal.

H Counterfactual Data Augmentation

To validate whether and to what extent counterfactual examples enhance model performance and robustness, we conduct counterfactual data augmen-

DeepSeek-R1-Distill-Llama-70B Evaluation

Original input: Johnson Back to His Best as D-Backs End Streak NEW YORK (Reuters) - Randy Johnson struck out 14 batters in 8 1/3 innings to help the Arizona Diamondbacks end a nine-game losing streak with a 2-0 win over the host New York Mets in the National League Sunday.

Label: sports

Counterfactual: Johnson Back to His Best as D-Backs End Streak <u>in Stock Market</u> NEW YORK (Reuters) - Randy Johnson struck out 14 <u>deals</u> in 8 1/3 <u>quarters</u> to help the Arizona Diamondbacks end a nine-game losing streak <u>in the stock market</u> with a 2-0 win over the host New York Mets in the National Exchange Sunday.

Chain of Thought: Alright, I'm trying to figure out how to classify this article into one of the four categories: world, sports, business, or science/technology. Let me read the input carefully.

Randy Johnson is a well-known baseball pitcher, so that's definitely a **sports** context. The content says "end a nine-game losing streak in the stock market". Wait, that's confusing because the stock market is related to business. Looking at the content, it says the Arizona Diamondbacks beating the New York Mets in the National Exchange Sunday. National Exchange could refer to a stock exchange. Therefore, the category should be **business**.

Figure 12: An example from AG News, its corresponding counterfactual generated by FIZLE, and the chain-of-thought from DeepSeek-R1-Distill-Llama-70B. <u>Underlines</u> indicate the insertion of new words, compared to the original input.

Model	Relation.	AG News	SST2	SNLI	Avg.	Model	Relation.	AG News	SST2	SNLI	Avg.
Llama3-8B	\mathcal{R}_{sm} \mathcal{R}_{dm} \mathcal{R}_{sf} \mathcal{R}_{imw} \mathcal{R}_{imwo} Ensemble	1 3 4 8 4.33 8	7 9 8 3 3.67 4	4 3 1 8 4.33 8	4 5 4.33 6.33 4.11 6.67	Llama3-8B	$egin{array}{c} \mathcal{R}_{sm} \ \mathcal{R}_{dm} \ \mathcal{R}_{sf} \ \mathcal{R}_{imw} \ \mathcal{R}_{imwo} \ ext{Ensemble} \end{array}$	2 3 6 8 3.33 8	9 1 3 5.5 5.67 4	7 8 3 5 5.33	6 4 6.17 4.78 4.33
Qwen2.5–14B	\mathcal{R}_{sm} \mathcal{R}_{dm} \mathcal{R}_{sf} \mathcal{R}_{imw} \mathcal{R}_{imwo} Ensemble	4 3 2 8 4 8	8 9 6 2 5.33 2	2 3 4 8 4 8	4.67 5 4 6 4.44 6	Qwen2.5-14B	$egin{array}{c} \mathcal{R}_{sm} \ \mathcal{R}_{dm} \ \mathcal{R}_{sf} \ \mathcal{R}_{imw} \ \mathcal{R}_{imwo} \ \mathcal{E}$ nsemble	6 5 4 8 2 8	8 9 7 3.5 3.33 4	4 8 7 3.5 5.33 3	7.33 6 5 3.55
Qwen2.5-32B	\mathcal{R}_{sm} \mathcal{R}_{dm} \mathcal{R}_{sf} \mathcal{R}_{imw} \mathcal{R}_{imwo} Ensemble	6 1 7 6.5 3.33 8	7 8 6 2.5 4.67 5	6 5 4 8.5 4 1	6.33 4.67 5.67 5.83 4 4.67	Qwen2.5-32B	$egin{array}{c} \mathcal{R}_{sm} \\ \mathcal{R}_{dm} \\ \mathcal{R}_{sf} \\ \mathcal{R}_{imw} \\ \mathcal{R}_{imwo} \\ ext{Ensemble} \end{array}$	5 4 2 8.5 3.33 7	6 9 8 2.5 4.33 4	4 8 5 4.5 4 7	5 7 5 5.17 3.89 6
Llama3-70B	\mathcal{R}_{sm} \mathcal{R}_{dm} \mathcal{R}_{sf} \mathcal{R}_{imw} \mathcal{R}_{imwo} Ensemble	3 4 2 8 4 8	9 7 6 4.5 3.67 3	2 3 5 8 6 1	4.67 4.67 4.33 6.83 4.56	Llama3-70B	\mathcal{R}_{sm} \mathcal{R}_{dm} \mathcal{R}_{sf} \mathcal{R}_{imw} \mathcal{R}_{imwo} Ensemble	6 4 2 8 3 8	8 9 2 6 2.67 6	4 8 3 3 6 6	6 7 2.33 5.67 3.89 6.67

⁽a) Counterfactual examples generated using FIZLE.

Table 3: The average ranking of judge-generator model relationship based on Δ in Table 4 (lower rankings indicate better alignment). Counterfactual examples are generated by Qwen2.5-{14B,32B} and Llama3-{8B,70B}, evaluated across judge models exhibiting **same**, distilled, **same** family, and independent **w**/ and **w**/o fine-tuning relationships on AG News, SST2 and SNLI. Green-highlighted values indicate that the judge model with the given relationship aligns **closely** with human annotators, while **red-highlighted** values indicate the **opposite**.

tation (CDA) experiments using a pretrained BERT model, LLM_C , without fine-tuning on any target dataset (§4.2). Note that the BERT model used for

the CDA experiment as $LLM_{\mathcal{C}}$ contrasts with the BERT model used as the judge model $LLM_{\mathcal{J}}$ (Table 3), which is fine-tuned on the target dataset. The

⁽b) Counterfactual examples generated using FLARE.

Model	Relation.	Judge Model (LLM,7)	AG News	SST2	SNLI	Model	Relation.	Judge Model ($LLM_{\mathcal{J}}$)	AG News	SST2	SNLI
	\mathcal{R}_{sm}	Llama3-8B	+15.36	-23.53	+27.00		\mathcal{R}_{sm}	Llama3-8B	+50.27	11.29	+34.86
	\mathcal{R}_{dm}	DeepSeek-R1-Distill-Llama-8B	+17.36	-27.13	+26.80		\mathcal{R}_{dm}	DeepSeek-R1-Distill-Llama-8B	+54.87	-1.10	+40.46
	\mathcal{R}_{sf}	Llama3-70B	+22.56	-25.53	+20.80		\mathcal{R}_{sf}	Llama3-70B	+64.47	+4.29	+29.26
m	\mathcal{R}_{imw}	BERT	+36.56	-15.33	+32.80	œ	\mathcal{R}_{imw}	BERT	+68.27	+8.77	+31.04
-8	\mathcal{R}_{imw}	RoBERTa	+37.56	-23.13	+35.80	8 - 8	\mathcal{R}_{imw}	RoBERTa	+68.07	+6.24	+29.77
Llama3-8B	\mathcal{R}_{imwo}	Phi4-14B	+15.56	-23.53	+26.80	Llama3-8B	\mathcal{R}_{imwo}	Phi4-14B	+56.07	+3.61	+28.50
Ľ	\mathcal{R}_{imwo}	Mistral-Large	+23.56	-21.13	+32.40	Ë	\mathcal{R}_{imwo}	Mistral-Large	+58.47	+9.34	+62.34
	\mathcal{R}_{imwo}	Gemini-1.5-pro	+28.32	-17.65	+30.60		\mathcal{R}_{imwo}	Gemini-1.5-pro	+39.43	+9.01	+30.60
	-	Ensemble	+37.56	-23.13	+35.80		-	Ensemble	+68.07	+6.24	+14.25
	-	User Study	75.56	46.67	100.00		-	User Study	86.67	73.33	100.00
	\mathcal{R}_{sm}	Qwen2.5-14B	+21.24	-28.62	+17.80		\mathcal{R}_{sm}	Qwen2.5-14B	46.93	-22.44	+32.29
	\mathcal{R}_{dm}	DeepSeek-R1-Distill-Qwen-14B	+20.64	-29.02	+18.40		\mathcal{R}_{dm}	DeepSeek-R1-Distill-Qwen-14B	+42.13	-24.16	+46.71
	\mathcal{R}_{sf}	Qwen2.5-72B	+17.04	-28.02	+21.20		\mathcal{R}_{sf}	Qwen2.5-72B	+41.93	-22.44	+36.05
4 B	\mathcal{R}_{imw}	BERT	+46.04	-23.02	+31.80	48	\mathcal{R}_{imw}	BERT	+53.53	-16.93	+30.09
2wen2.5-14В	\mathcal{R}_{imw}	RoBERTa	+43.84	-24.02	+38.60	ეwen2.5−14B	\mathcal{R}_{imw}	RoBERTa	+53.13	-19.00	+33.23
٦2.	\mathcal{R}_{imwo}	Phi4-14B	+14.84	-27.62	+13.80	n2.	\mathcal{R}_{imwo}	Phi4-14B	+41.13	-22.44	+33.23
Me	\mathcal{R}_{imwo}	Mistral-Large	+27.04	-28.42	+22.00]wei	\mathcal{R}_{imwo}	Mistral-Large	+40.73	-12.46	+54.55
0	\mathcal{R}_{imwo}	Gemini-1.5-pro	+22.13	-26.62	+27.20	O O	\mathcal{R}_{imwo}	Gemini-1.5-pro	+11.02	-17.75	+27.20
	-	Ensemble	+43.84	-24.02	+32.02		-	Ensemble	+53.13	-19.00	+33.23
	-	User Study	84.44	57.78	100.00		-	User Study	73.33	66.67	100.00
	\mathcal{R}_{sm}	Qwen2.5-32B	-10.33	-22.13	+30.00		\mathcal{R}_{sm}	Qwen2.5-32B	+38.31	-35.36	+32.54
	\mathcal{R}_{dm}	DeepSeek-R1-Distill-Qwen-32B	-0.53	-22.33	+25.60		\mathcal{R}_{dm}	DeepSeek-R1-Distill-Qwen-32B	+37.71	-39.49	+50.36
	\mathcal{R}_{sf}	Qwen2.5-72B	-16.21	-21.73	+23.80		\mathcal{R}_{sf}	Qwen2.5-72B	+35.91	-37.54	+34.68
œ	\mathcal{R}_{imw}	BERT	+9.62	-19.53	+33.00	2B	\mathcal{R}_{imw}	BERT	+47.91	-31.92	+30.64
-32	\mathcal{R}_{imw}	RoBERTa	+27.62	-15.13	+38.20	5-3	\mathcal{R}_{imw}	RoBERTa	+47.41	-32.26	+34.92
2.5	\mathcal{R}_{imwo}	Phi4-14B	-3.98	-22.93	+15.80	n2.	\mathcal{R}_{imwo}	Phi4-14B	+36.71	-36.39	+30.64
2wen2.5-32B	\mathcal{R}_{imwo}	Mistral-Large	+10.22	-18.13	+22.60	Qwen2.5-32В	\mathcal{R}_{imwo}	Mistral-Large	+38.91	-24.92	+53.21
ð	\mathcal{R}_{imwo}	Gemini-1.5-pro	+3.40	-18.76	+30.60	0	\mathcal{R}_{imwo}	Gemini-1.5-pro	+12.29	-34.32	+30.60
	-	Ensemble	+27.62	-20.93	+12.80		-	Ensemble	+47.31	-32.26	-34.92
	-	User Study	62.22	66.67	100.00		-	User Study	71.11	51.11	100.00
	\mathcal{R}_{sm}	Llama3-70B	+1.84	-43.38	+16.40		\mathcal{R}_{sm}	Llama3-70B	+39.13	-25.05	+36.52
	\mathcal{R}_{dm}	DeepSeek-R1-Distill-Llama-70B	+3.84	-41.70	+18.40		\mathcal{R}_{dm}	DeepSeek-R1-Distill-Llama-70B	+34.73	-27.11	+44.58
	\mathcal{R}_{sf}	Llama3-8B	-1.76	-40.58	+26.20		\mathcal{R}_{sf}	Llama3-8B	+26.53	-12.09	+33.25
70B	\mathcal{R}_{imw}	BERT	+18.24	-36.98	+31.40	0B	\mathcal{R}_{imw}	BERT	+42.13	-22.53	+30.48
3-7	\mathcal{R}_{imw}	RoBERTa	+21.24	-36.78	+37.40	3-7	\mathcal{R}_{imw}	RoBERTa	+39.73	-23.67	+37.53
lama3-70B	\mathcal{R}{imwo}	Phi4-14B	+0.84	-42.38	+22.80	.lama3-70B	\mathcal{R}_{imwo}	Phi4-14B	+33.53	-20.69	+37.78
Ľ	\mathcal{R}_{imwo}	Mistral-Large	+11.64	-31.38	+29.80	Ë	\mathcal{R}_{imwo}	Mistral-Large	+37.53	-11.63	+47.60
	\mathcal{R}_{imwo}	Gemini-1.5-pro	-10.67	-35.17	+31.40		\mathcal{R}_{imwo}	Gemini-1.5-pro	+19.56	-15.17	+31.40
	-	Ensemble	+21.24	-36.78	+9.80		-	Ensemble	+39.73	-23.67	+37.53
	-	User Study	64.44	42.22	100.00		-	User Study	73.33	62.22	100.00

⁽a) Counterfactual examples generated using FIZLE.

(b) Counterfactual examples generated using FLARE.

Table 4: The LFR difference ($\Delta\%$) between the user study and the judge–generated model relationships (with values closer to 0 indicating better alignment). Counterfactual examples are generated by Qwen2.5-{14B,32B} and Llama3-{8B,70B}, evaluated across judge models exhibiting same, distilled, same family, and independent w/ and w/o fine-tuning relationships on AG News, SST2 and SNLI. The user study to assess the LFR is conducted on 45 selected counterfactuals (§4.4). Red-highlighted values indicate that the judge model with the given relationship aligns closely with human annotators, while green-highlighted values indicate the opposite.

training set for fine-tuning the BERT model $(LLM_{\mathcal{C}})$ consists of 500 randomly selected instances from the original training set, along with their corresponding counterfactual examples generated by the generator model $(LLM_{\mathcal{G}})$, with labels assigned by various judge models $(LLM_{\mathcal{J}})$. Our baseline is a BERT model $(LLM_{\mathcal{B}})$, which is fine-tuned only on the same 500 randomly selected instances from the original training set.

H.1 Evaluation on the original test set

Table 6 presents the accuracy of the BERT model (LLM_C) augmented with additional counterfactual examples. Both evaluations are performed on the **original test set** of each dataset (§4.2). We observe that, through CDA, the performance of the BERT

model $(LLM_{\mathcal{C}})$ improves noticeably compared to the baseline BERT model $LLM_{\mathcal{B}}$, by up to 15.13% on average. BERT and RoBERTa, as $LLM_{\mathcal{J}}$, generally provide the most efficient labels for augmentation across the AG News and SST2 datasets. This may be ascribable to the fact that the BERT and RoBERTa used as the judge models $(LLM_{\mathcal{J}})$ and the BERT model used for CDA $(LLM_{\mathcal{C}})$ share the same or similar architecture, and thus, the labels provided by judge models $LLM_{\mathcal{J}}$ offer $LLM_{\mathcal{C}}$ a greater advantage compared to labels from judge models with other relationships.

Meanwhile, the performance gains observed when comparing $LLM_{\mathcal{B}}$ and $LLM_{\mathcal{C}}$, attributable to counterfactuals generated by $LLM_{\mathcal{G}}$, vary across tasks: Llama3-70B generates the most effective

Model	Judge Model ($LLM_{\mathcal{J}}$)	AG News	SST2	SNLI	Model	Judge Model ($LLM_{\mathcal{J}}$)	AG News	SST2	SNLI
	Llama3-8B	60.20	70.20	75.55		Llama3-8B	42.22	80.00	64.44
	DeepSeek-R1-Distill-Llama-8B	58.20	73.80	71.11		DeepSeek-R1-Distill-Llama-8B	40.00	82.22	55.55
Ω.	Llama3-70B	53.00	72.20	82.22	<u>m</u>	Llama3-70B	33.33	73.33	73.33
3-8	BERT	39.00	62.00	71.11	3-8	BERT	15.55	71.11	77.77
Llama3-8B	RoBERTa	38.00	69.80	62.22	Llama3-8B	RoBERTa	17.77	73.33	75.55
Ľ	Phi4-14B	60.00	70.20	68.88	Ľ	Phi4-14B	40.00	80.00	80.00
	Mistral-Large	52.00	67.80	62.22		Mistral-Large	31.11	75.55	80.00
	User Study	75.56	46.67	100.00		User Study	86.67	73.33	100.00
	Qwen2.5-14B	57.77	93.33	84.44		Qwen2.5-14B	26.66	88.88	62.22
	DeepSeek-R1-Distill-Qwen-14B	63.80	95.55	91.11		DeepSeek-R1-Distill-Qwen-14B	33.33	93.33	53.33
Qwen2.5–14B	Qwen2.5-72B	68.88	97.77	80.00	48	Qwen2.5-72B	37.77	91.11	66.66
5-1	BERT	26.66	86.66	73.33	2-1	BERT	15.55	86.66	64.44
n2 .	RoBERTa	26.66	86.66	57.77	Qwen2.5-14B	RoBERTa	17.77	86.66	71.11
Me	Phi4-14B	71.11	93.33	86.66		Phi4-14B	31.11	91.11	60.00
O	Mistral-Large	62.22	93.33	82.22		Mistral-Large	37.77	79.13	71.11
	User Study	84.44	57.78	100.00		User Study	73.33	66.67	100.00
	Qwen2.5-32B	60.00	91.11	71.11		Qwen2.5-32B	37.77	86.66	57.77
	DeepSeek-R1-Distill-Qwen-32B	62.75	88.88	71.11		DeepSeek-R1-Distill-Qwen-32B	33.33	88.88	42.22
32B	Qwen2.5-72B	62.22	91.11	77.77	22B	Qwen2.5-72B	35.55	91.11	55.55
5-3	BERT	31.11	84.44	71.11	5-	BERT	13.33	84.44	64.44
n2.	RoBERTa	33.33	84.44	57.77	n2.	RoBERTa	20.00	84.44	53.33
Qwen2.5-32B	Phi4-14B	71.11	88.88	82.22	Qwen2.5-32B	Phi4-14B	33.33	88.88	53.33
O	Mistral-Large	66.66	86.66	84.44	O	Mistral-Large	31.11	77.77	51.11
	User Study	62.22	66.67	100.00		User Study	71.11	51.11	100.00
	Llama3-70B	62.60	85.60	84.44		Llama3-70B	35.55	91.11	62.22
	DeepSeek-R1-Distill-Llama-70B	60.60	83.92	86.66		DeepSeek-R1-Distill-Llama-70B	38.60	86.66	46.66
0B	Llama3-8B	66.20	82.80	71.11	0B	Llama3-8B	57.77	86.66	64.44
3-7	BERT	46.20	79.20	73.33	Llama3-70B	BERT	44.44	86.66	75.55
Llama3-70B	RoBERTa	43.20	79.00	62.60	ama.	RoBERTa	37.77	86.66	60.00
Lla	Phi4-14B	63.60	84.60	73.33	Lla	Phi4-14B	44.44	91.11	60.00
	Mistral-Large	52.80	73.60	75.55		Mistral-Large	35.55	75.55	60.00
	User Study	64.44	42.22	100.00		User Study	73.33	62.22	100.00

⁽a) Counterfactual examples generated using FIZLE.

(b) Counterfactual examples generated using FLARE.

Table 5: Label flip rate (in %) for counterfactual examples generated by Qwen2.5-{14B,32B} and Llama3-{8B,70B}, evaluated across judge models exhibiting same, distilled, same family, and independent w/ and w/o fine-tuning relationships, and user study on 45 selected counterfactuals (§4.4) each from AG News, SST2 and SNLI datasets. Orange-highlighted values indicate that the judge model with the given relationship aligns closely with human annotators, while purple-highlighted values indicate the opposite.

counterfactual instances on AG News with averaged accuracy of 0.85, while Qwen2.5-7B is the most effective on SST2, but it is the least effective on SNLI. The independent, non-fine-tuned relationship achieves the most closely aligned flip rate based on the user study. As a result, this relationship yields the best performance in counterfactual data augmentation on the AG News and SST2 datasets.

H.2 Evaluation on the counterfactual set

In comparison to Section §H.1, where $LLM_{\mathcal{B}}$ and $LLM_{\mathcal{C}}$ are evaluated on the test set of each dataset, we further evaluate the fine-tuned BERT model $LLM_{\mathcal{C}}$ for CDA on the set of 45 selected counterfactuals, whose labels are obtained through the user study (§4.4). Note that the 45 selected counterfactuals and their corresponding original input

texts are excluded from the training data for the model.

Table 6 illustrates the performance of the BERT model $LLM_{\mathcal{C}}$ after fine-tuning, evaluated on the selected counterfactuals with human-annotated labels. Similar to Section 5, we count the number of instances in which $LLM_{\mathcal{J}}$ models with a specific relationship most closely or least align with human evaluation results across the three datasets. Table 6 outlines that the judge model $LLM_{\mathcal{J}}$ with an independent relationship without fine-tuning on the target dataset proves to be the most effective configuration for evaluating the validity of counterfactuals generated by LLM_G , which aligns with, and further validates, our findings in Section 5 (Table 3). Additionally, our findings further indicate that $LLM_{\mathcal{J}}$, when configured with an independent relationship and no fine-tuning on the target dataset,

36.11		Origi	nal Test S	et	C	CF Set			
Model	Judge Model	AG News	SST2	SNLI	AG News	SST2	SNLI		
	Without CDA (Baseline)	0.766	0.779	0.562	0.307	0.516	0.289		
	Meta-Llama-3-8B-Instruct	0.837	0.809	0.644	0.267	0.553	0.311		
rct	DeepSeek-R1-Distill-Llama-8B	0.842	0.804	0.626	0.296	0.586	0.244		
Llama3-8B-Instruct	Meta-Llama-3-70B-Instruct	0.833	0.8337	0.633	0.278	0.588	0.276		
Į-	BERT	0.855	0.864	0.595	0.284	0.583	0.338		
3-8	RoBERTa	0.869	0.873	0.604	0.281	0.583	0.240		
ama	Phi4-14B	0.838	0.844	0.619	0.264	0.573	0.360		
Ξ	Mistral-Large-Instruct	0.843	0.803	0.627	0.251	0.560	0.293		
	Qwen2.5-14B-Instruct	0.845	0.817	0.637	0.281	0.578	0.364		
ruci	DeepSeek-R1-Distill-Qwen-14B	0.837	0.822	0.621	0.274	0.546	0.258		
nsti	Qwen2.5-72B-Instruct	0.838	0.811	0.656	0.291	0.561	0.280		
1-8+	BERT	0.857	0.857	0.600	0.274	0.558	0.316		
Qwen2.5-14B-Instruct	RoBERTa	0.869	0.791	0.632	0.284	0.550	0.262		
.n2.	Phi4-14B	0.825	0.825	0.629	0.284	0.576	0.338		
Owe Owe	Mistral-Large-Instruct	0.803	0.788	0.642	0.257	0.542	0.222		
ш	Qwen2.5-32B-Instruct	0.813	0.836	0.646	0.277	0.547	0.347		
LON.	DeepSeek-R1-Distill-Qwen-32B	0.842	0.836	0.648	0.286	0.533	0.351		
nst	Qwen2.5-72B-Instruct	0.774	0.831	0.646	0.264	0.532	0.316		
Qwen2.5-32B-Instruct	BERT	0.788	0.852	0.594	0.247	0.540	0.351		
5-37	RoBERTa	0.866	0.853	0.644	0.274	0.569	0.267		
n2.	Phi4-14B	0.856	0.827	0.653	0.301	0.540	0.396		
Owe Owe	Mistral-Large-Instruct	0.831	0.780	0.631	0.269	0.523	0.298		
	Meta-Llama-3-70B-Instruct	0.853	0.803	0.606	0.267	0.595	0.347		
.nc.t	DeepSeek-R1-Distill-Llama-70B	0.856	0.803	0.629	0.267	0.570	0.267		
ıstr	Meta-Llama-3-8B-Instruct	0.846	0.820	0.624	0.286	0.575	0.307		
B-Ir	BERT	0.874	0.820	0.612	0.254	0.600	0.324		
-70	RoBERTa	0.853	0.853	0.629	0.247	0.595	0.320		
Llama3-70B-Instruct	Phi4-14B	0.857	0.812	0.638	0.267	0.570	0.369		
	Mistral-Large-Instruct	0.859	0.791	0.663	0.235	0.568	0.289		

Table 6: Downstream task performance (measured in terms of accuracy) is evaluated on *test set* and *the set of counterfactuals (out-of-distribution instances)* after applying counterfactual data augmentation on a BERT model (LLM_C). The training data consist of original examples from the target dataset, along with counterfactual examples generated by Qwen2.5-{14B,32B} and Llama3-{8B,70B} using FIZLE. The counterfactual labels are provided by different judge models exhibiting various relationships: same model, distilled, same family, and independent models with fine-tuning or without fine-tuning, across the AG News, SST2, and SNLI datasets.

generally provides LFR most closely aligned with those from human evaluation. This setup enables more effective and valid predicted labels for generated counterfactuals, which in turn contributes to better-performing and more robust models.

We calculate the Spearman correlation between the rankings of the generator and judge models in Table 3 and Table 6 (CF set). The results show a moderate correlation of 0.41 on the AG News dataset, indicating that the relationships might impact the performance of the CAD. Specifically, a better relationship may lead to higher accuracy on the CF test set. In contrast, a weak correlation is observed on other datasets.